

COMPUTER-AIDED SIMULATION OF UNMANNED AERIAL VEHICLE COMPOSITE STRUCTURE DYNAMICS

Artur KIERZKOWSKI¹, Tomasz KISIEL¹, Maciej MILEWSKI¹✉, Ádám TÖRÖK²✉, Michał STOSIAK¹✉, Jakub WRÓBEL¹

¹Dept of Technical Systems Operation and Maintenance, Faculty of Mechanical Engineering, Wrocław University of Science and Technology, Poland

²Dept of Transport Technology and Economics, Faculty of Transportation Engineering and Vehicle Engineering, Budapest University of Technology and Economics, Hungary

Highlights:

- a numerical model was developed using ANSYS software and the ACP module to simulate the dynamic response of a composite plate with varying fibre orientations;
- simulations were conducted for fibre orientations at 0°, 30°, 45°, and 90°, showing significant differences in natural frequencies and mode shapes;
- the dynamic response of a homogenous material was compared with material in which fibre directionality was considered, highlighting the influence of fibre orientation on the structure's dynamic properties;
- the study confirmed that considering fibre directionality is essential for accurate dynamic simulations, especially for UAV structures.

Article History:

- submitted 15 October 2024;
- resubmitted 14 November 2024;
- accepted 5 December 2024.

Abstract. The dynamic response of an aerial vehicle structure is a key parameter that must be determined before further aeroelastic phenomena can be analysed in the aerospace sector. Natural frequencies, mode shapes, and damping can be measured or predicted through experimental, operational, or computational studies. To reduce the costs and complexity of experimental investigations, there is a demand for numerical models that accurately represent the structure's dynamic behaviour. This article focuses on modelling composite structures, which are increasingly utilised in the aerospace industry and whose dynamic properties are heavily influenced by fibre directionality. ANSYS software and the ACP module were employed to develop a numerical model of a wet Epoxy Carbon UD (230 GPa) composite commonly used in Unmanned Aerial Vehicle (UAV) components. Ten layers of 0.1 mm thick carbon fibre were incorporated into the model to create a 1 mm thick composite plate, with fibres oriented at 0°, 30°, 45°, and 90° relative to the horizontal direction of the plate. The simulations demonstrated that careful consideration and modelling of the material significantly impact the values of natural frequencies and, more importantly, the mode shapes.

Keywords: unmanned aerial vehicle, modal analysis, composite, finite element method, vibration.

✉ Corresponding author. E-mail: maciej.milewski@pwr.edu.pl

✉ Editor of the TRANSPORT – the manuscript was handled by one of the Associate Editors, who made all decisions related to the manuscript (including the choice of referees and the ultimate decision on the revision and publishing).

Notations

ACP – ANSYS composite <i>PrepPost</i> ;	FEM – finite element method;
CFD – computational fluid dynamics;	GFRP – glass fibre-reinforced polymer;
CFRP – carbon fibre-reinforced polymer;	GVT – ground vibration testing;
CLT – classical laminate theory;	NFC – natural fibre composite;
CNT – carbon nanotube;	ROM – reduced-order model;
DIC – digital image correlation;	SAR – search and rescue;
DOF – degree of freedom;	UAV – unmanned aerial vehicle;
EMA – experimental modal analysis;	UD – unidirectional.

1. Introduction

UAVs are aircraft specifically designed and equipped for flight without a pilot onboard (ICAO 2011). The origins of UAV technology are deeply rooted in the military domain; however, their remarkable versatility has rapidly led to widespread adoption in both scientific and commercial sectors (Kovalev *et al.* 2019; Herrick 2000). In recent years, the drone market has experienced significant growth, driven by increasing demand and evolving societal needs. Currently, UAVs are extensively employed in terrain mapping, geological research, archaeological excavation, agriculture, and forestry, where they monitor crop health, document damage, and detect plant diseases (Bagdi *et al.* 2023). Moreover, drones have assumed a critical role in SAR operations. UAVs are utilised in various sectors due to their versatility. Crop monitoring and precision farming, optimising resource use through detailed data collection, is used in agriculture (Anderson, Gaston 2013; Zhang, Kovacs 2012). Another significant application is environmental monitoring, which facilitates wildlife conservation and effective disaster management by acquiring high-resolution aerial data (Rose *et al.* 2015; Bushnaq *et al.* 2022). In infrastructure inspection, UAVs provide a safe and cost-effective alternative for evaluating structural integrity, including the assessment of bridges, power lines, and oil and gas pipelines (Ciampa *et al.* 2019; Hausamann *et al.* 2005).

Furthermore, UAVs are integral to mapping and surveying applications, enabling the production of accurate topographic maps and detailed 3-dimensional models (Colomina, Molina 2014; Rango *et al.* 2009). In emergency response scenarios, UAVs assist in SAR operations by delivering real-time aerial imagery, particularly valuable in challenging terrain conditions (Lyu *et al.* 2023). The applicability of UAV technology extends to logistics, where they are being evaluated for package delivery in both remote and urban environments, potentially transforming supply chain dynamics (Zrelli *et al.* 2024). In military and defence operations, UAVs are employed for surveillance, reconnaissance, and target acquisition, fundamentally altering the landscape of modern warfare (Malinowski 2016; Koukoudakis 2024). Collectively, these applications demonstrate that UAV technology enhances operational efficiency, safety, and data collection capabilities across diverse scientific and practical fields.

The increasing use of composite materials in modern aircraft and UAV design introduces unique challenges in structural analysis. Flutter is one of the most dangerous phenomena, which occurs when aerodynamic forces interact with a structure's natural vibration frequencies (Dinulović *et al.* 2024; Stosiak *et al.* 2022). Unlike traditional metallic materials, composites exhibit orthotropic and heterogeneous characteristics, significantly complicating vibration prediction. The frequency response analysis method is often used to determine nonlinear characteristics (Karpenko, Nugaras 2022). As a complement, a FEM is used for numerical simulation, in combination with experimental measurements based on frequency response

optimisation, to model the behaviour of an element made of composite material (Karpenko *et al.* 2023). The issues of dynamic in-flight behaviour of the wing are crucial for flight stability and safety, and safety requirements are key in the aerospace industry (Karpenko 2022). This article focuses on demonstrating the impact of fibre reinforcement orientation in laminates on the modal characteristics of structures. It emphasises the necessity of considering this orientation during the simulation modal analysis of composites – critical for their implementation in the aerospace industry. The aircraft design process aims to reduce weight.

Additionally, due to the desire to minimise aerodynamic drag, wings with increasing aspect ratios are being developed. The UAV wing has different behaviour depending on the changing flight conditions and requires a detailed design to obtain the best aerodynamic performance. The difficult task is the need to simultaneously satisfy 2 conditions Bishay & Aguilar (2021) considered to conflict with each other: high in-plane stiffness and good damping properties. Therefore, the wing skin must be stiff enough to withstand the aerodynamic loads of the wind (Bubert *et al.* 2010) while providing sufficient damping of wind-induced vibrations during UAV flight (George *et al.* 2021). A balance is aimed at the wings' weight, stiffness, and aerodynamic performance (Kontogiannis, Ekaterinaris 2013). Aeroelastic tailoring is crucial for maximising UAV performance (Weisshaar *et al.* 1998). Aeroelastic phenomena in UAVs are significantly nonlinear due to their lightweight structures, high aspect ratios, and the prevalent use of composite materials in wing design. Investigating these nonlinear behaviours has become a focus of numerous studies integrating simulation and experimental approaches (Bras *et al.* 2022; Patil 2003; Körpe, Kanat 2019). The low weight and significant wingspan are associated with significant deformations under load. These deformations alter the distribution of aerodynamic forces, which varies based on the extent of deformation (Garrick, Reed 1981). This feedback leads to flutter, which, as previously mentioned, occurs when aerodynamic forces interact with the natural frequencies of the aircraft structure. Phenomena such as flutter are part of the science of aeroelasticity. Aeroelasticity studies the interaction among aerodynamic, inertial, and structural elastic forces acting on an elastic body as fluid flows around it (Hodges, Pierce 2011).

Since most contemporary flutter analysis methods are based on the modal superposition approach, it is essential to determine the natural frequencies of the aircraft, treated as a free (unconstrained) object. Therefore, modal analysis of the structure is the initial step in aeroelastic studies. These natural frequencies can be determined using a computational numerical model or measured through EMA (Chajec 2020).

Composite materials, particularly carbon-epoxy laminates, are widely used across various transportation sectors (Kootatp *et al.* 2023; Rangappa *et al.* 2020) due to their superior mechanical properties, such as a high strength-

to-weight ratio and stiffness, which directly influence natural frequencies. Example applications in automotive and aerospace sectors are presented in Figure 1. Composite materials are engineered substances, either synthesised from 2 or more distinct materials with varying physical and chemical properties or derived by combining their characteristics to produce a material with enhanced or novel properties compared to its components. One constituent, the reinforcement, is typically embedded within a secondary component called the matrix. Reinforcements are often fibrous, as fibres are mainly responsible for carrying mechanical loads. Conversely, the matrix maintains the spatial integrity of the fibres, protecting them from mechanical degradation or chemical corrosion (Mallick 2007).

In the aerospace sector, laminated composites are particularly common. These materials consist of multiple layers, or plies, that are permanently bonded to form a cohesive structural system. The arrangement and bonding of these layers contribute significantly to overall mechanical performance, providing superior strength-to-weight ratios, stiffness, and resistance to various forms of environmental and operational damage. The vibrational response of aircraft structures is crucial, especially during dynamic loading conditions such as take-off, landing, and turbulent flight. Traditional, isotropic metallic structures exhibit a well-understood vibrational profile due to their uniform material properties. However, composite materials introduce significant complexity in vibration analysis due to their orthotropy. Specifically, composites exhibit directionally dependent stiffness and strength characteristics, directly influencing their natural frequencies, mode shapes, and damping properties (Gibson 2016; Kollár, Springer 2003). One primary concern in the modal analysis of composite structures is the resonance frequency. In metallic structures, the modes are generally predictable and can be controlled through design modifications. How-

ever, the inherent orthotropy of composite materials can result in non-intuitive modes and resonance phenomena that are more challenging to predict and avoid (Gibson 2016; Davies, Zhang 1995). These resonance conditions can lead to structural fatigue, delamination, and ultimately catastrophic aircraft failure (Schaff, Davidson 1997). Experimental techniques, such as modal analysis, are widely used to determine composite structures' natural frequencies, mode shapes, and damping ratios. These methods typically involve exciting the material using a hammer or shaker and measuring the response with accelerometers or laser vibrometers. Tremaine (2012) conducted EMA on composite plates with damping materials, combining experimental and analytical approaches to validate dynamic properties. Moreover, advanced optical techniques like DIC and fibre Bragg gratings have captured high-frequency responses in aerospace composites (Panopoulou *et al.* 2011).

In parallel, the FEM is extensively applied to simulate the dynamic response of composites. FEM allows for detailed modelling of the orthotropic and heterogeneous nature of these materials, making it a powerful tool for predicting natural frequencies, mode shapes, and stress distributions under dynamic loads (Ficzere 2022). However, the accuracy of FEM depends heavily on input parameters and model calibration. Often, FEM models tend to overestimate stiffness, making experimental validation essential. Studies by Friswell & Mottershead (1995) and Pálfi & Ficzere (2025) emphasise the importance of updating FEM models with experimental data to improve simulation accuracy. Recent research has focused on integrating experimental data with FEM simulations to enhance the identification of dynamic properties. Noman *et al.* (2023) investigated the effect of fibre orientation on the mechanical properties of carbon fibre composites under tensile loading and in dynamic response analysis. Their study modelled laminated carbon fibre composites using

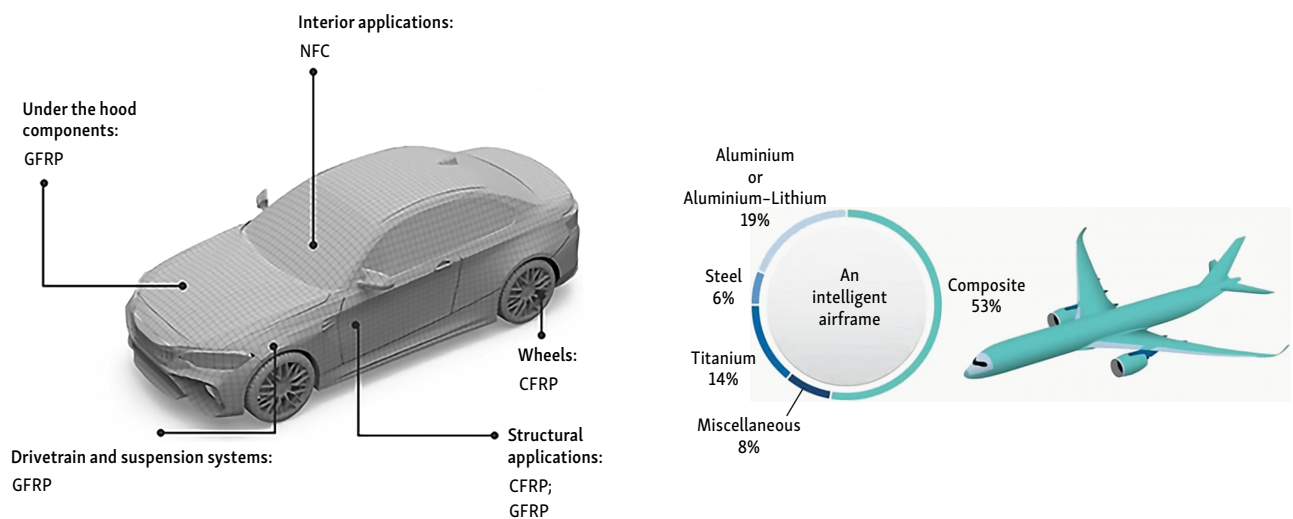


Figure 1. Applications of composite materials in transportation sectors (adopted by authors from Addcomposites 2024; Gondaliya *et al.* 2016)

ACP. Qaumi & Hashemi (2023) verified the accuracy of numerical models for composite rocket structures with EMA. In their research, numerical simulations were performed in ANSYS, and experiments were conducted using a hammer tap test with laser vibrometers as sensors. In summary, the literature highlights that the modal analysis of composite materials in aerospace continues to be a dynamic research area, driven by the ongoing pursuit of optimal testing conditions and accurate computer models. This article contributes to the field by presenting the impact of proper modelling of composite structures on the results of modal analysis simulations.

2. Modal analysis

The modal analysis is the fundamental dynamic analysis of a structure, focused on determining its natural frequencies, mode shapes, and damping properties. These parameters describe the structure's response to excitations and are essential for understanding and modifying its dynamic behaviour. The equation that describes the system motion is (Ewins 2000):

$$[M] \cdot \{\ddot{q}\} + [C] \cdot \{\dot{q}\} + [K] \cdot \{q\} = \{F(t)\}, \quad (1)$$

where: $[M]$, $[C]$ and $[K]$ represent mass, damping and stiffness matrices (in the case of composite materials, the matrices are derived using CLT (Nettles 1994)); $\{q\}$ is the vector of displacements; $\{\dot{q}\}$ is the vector of velocities; $\{\ddot{q}\}$ is the vector of accelerations; $\{F(t)\}$ is the vector of external forces applied to the structure and varies depending on the excitation type (time – dependent loads, harmonic excitation, impulsive loads, distributed loads).

If external load effects and damping effects are not considered, the equation becomes:

$$[M] \cdot \{\ddot{q}\} + [K] \cdot \{q\} = 0, \quad (2)$$

when harmonic motion is assumed:

$$\{q\} = \{\varphi_i\} \cdot \sin(\omega_i \cdot t + \theta_i); \quad (3)$$

$$\{\ddot{q}\} = -\omega_i^2 \cdot \{\varphi_i\} \cdot \sin(\omega_i \cdot t + \theta_i), \quad (4)$$

where: φ_i is amplitude corresponding to the i th mode; ω_i is angular frequency for the i th mode; θ_i is initial phase for the i th mode; t is a point in time after release from the initial position; the roots ω_i^2 of the equation represent eigenvalues, which are the square of the natural circular frequency of the structure ω_i .

Substitution $\{q\}$ and $\{\ddot{q}\}$ in the governing equation gives an eigenvalue equation:

$$([K] - \omega_i^2 \cdot [M]) \cdot \{\varphi_i\} = \{0\}. \quad (5)$$

Subsequently, let the determinant equals zero, and the eigenvalue problem is solved by:

$$\det([K] - \omega_i^2 \cdot [M]) = \{0\}. \quad (6)$$

2.1. Simulation modal analysis

The FEM and computational models, developed based on geometric models, are commonly used for simulation modal analysis. It is crucial to accurately define the materials, mass distribution, connections, and boundary conditions of the analysed object. The frequencies, mode shapes, and damping coefficients determined through this method are fundamental for subsequent aeroelastic analyses. In the aerospace sector, beam models are typically used for calculations; however, in some cases, their limitations may prevent their application (Chajec 2018). These models significantly simplify the structure, potentially neglecting geometric complexity, mass distribution, or nonlinearities. Alternative modelling approaches can address some of these deficiencies, but they too come with limitations. Enhanced Beam Models, which incorporate shear deformation or rotational inertia can improve accuracy for flexible structures but are still constrained by the simplified assumptions of beam theory (Kidane, Troiani 2020). These models fail to capture 3-dimensional stress distributions and local deformations, which can be critical in aeroelastic contexts involving complex load paths or localized effects. FEM-based aeroelastic models provide a higher level of fidelity by integrating detailed structural and aerodynamic interactions, sometimes coupling with CFD for a more accurate representation of the aeroelastic loads (Piccione *et al.* 2012). However, these models are extremely computationally expensive, especially for large structures like wings or entire aircraft, and are not always feasible for iterative design processes or real-time aeroelastic simulations. FEM-based aeroelastic models can also suffer from numerical instabilities and require careful validation, as small inaccuracies in setup can lead to significant deviations in predicted flutter speeds or response to aerodynamic loads. Aeroelastic ROMs attempt to balance accuracy and efficiency by simplifying high-fidelity models into forms that retain the essential dynamic characteristics. ROMs are used to approximate complex aeroelastic behaviour in a computationally efficient way (Silva 2007). Yet, despite these simplifications, ROMs often fail to fully capture nonlinear aeroelastic effects, such as limit cycle oscillations, and may struggle with accuracy under varying flight conditions or high-amplitude structural responses. The computed results may contain errors and, as a result, may deviate from empirical data. Therefore, combining computational results with measurements is recommended to identify key elements of the model or assumed simulation parameters that influence the obtained results. Refining the model to align measured and simulated values enables the implementation of improved solutions in subsequent analyses, thereby increasing the reliability of the results (Dagilis, Kilikevicius 2023; Rahmani *et al.* 2013). As the design process progresses, models are continuously refined and verified. A reliable computational model allows for various calculations, even for different aircraft configurations, without requiring iterative structural testing for every modification. Based on these models, it is also possible to assess the

sensitivity of results to changes in structural parameters. However, in this study, experimental validation was not conducted, as it will be part of future work.

2.2. EMA

EMA, or GVT, aims to test and verify critical flutter simulation results and reduce the risk associated with flight flutter tests. GVT is required for new aircraft development programs and in cases of significant structural modifications to existing programs or new store configurations for military aircraft. Modal testing on the full aircraft helps calibrate computer-based finite element models for further flutter predictions (Siemens 2022). GVT is typically performed late in the development cycle once the fully integrated aircraft is ready.

During GVT, the aircraft is typically lifted off the ground using a soft suspension system that simulates a free-free condition. The goal is to ensure good separation between the rigid body modes and the 1st flexible mode. However, the introduction of a suspension system can add a slight degree of stiffness and damping to the setup. This added stiffness could slightly alter the rigid body mode frequencies, potentially influencing the mode separation critical for subsequent analysis. To minimize these effects, the characteristics of the suspension system must be chosen carefully. The selection is typically based on the aircraft's specific mass distribution and structural stiffness. As a practical criterion for effective suspension, it is generally accepted that the highest frequency of the aircraft, treated as a rigid body on the suspension compliance should be at least 3 times lower than the lowest natural frequency on the deformable aircraft (Chajec 2020). This ensures that the highest suspension frequency remains well below the lowest resonant frequency targeted in the measurement. When it is not possible to suspend large aircraft flexibly, air cushions are placed under the landing gear. An appropriate aircraft configuration must be selected for the tests, including its load and the configuration of all structural elements (Chajec 2020). The aircraft's propulsion system is inactive during the measurements. Vibrations are excited at one or several points using electrodynamic shakers, typically attached to the wings, tail, and possibly the fuselage. Accelerometers are then used to measure the vibration modes.

3. Modal analysis of composite structure

Most modern aviation structures, particularly UAVs, are made of laminates. The most popular materials are CFRPs, valued for their high strength-to-weight ratio, which makes them ideal for structural components such as frames, wings, and frames. GFRPs serve as a cost-effective alternative, offering adequate mechanical properties where high strength is needed at a lower cost. However, they exhibit reduced strength compared to carbon composites. Aramid fibre composites, such as Kevlar, are selected for their superior impact resistance, making them suitable for

applications requiring enhanced protection, such as collision shields or protective housings. Hybrid composites, which combine various fibre types, enable fine-tuning of mechanical characteristics to meet specific structural demands, such as varying load conditions across different UAV components. CNT-based composites provide exceptional mechanical properties, such as high tensile strength and low density, but elevated production costs currently constrain their application. Thermoplastic composites, though less mechanically robust than thermoset alternatives, are frequently utilised in non-critical UAV components due to their lower cost, ease of processing, and favourable environmental resistance. The selection of composite materials in UAV design is driven by a balance of mechanical performance, weight reduction, aerodynamic optimisation, and cost-effectiveness, with CFRP being the most commonly used due to its superior properties. However, GFRP and hybrid composites also find application in scenarios where cost constraints and specific material properties necessitate their use.

In this study, composite modelling and modal analysis are presented. The ANSYS software was used for this purpose. The ACP module was employed for composite modelling. It enables the modelling of composites layer by layer. The material of each layer, its orientation, and the stack-up sequence can be defined. The Modal module was used for the modal analysis, utilising different solvers to perform the modal analysis. The geometry of the analysed structure is a simple 500 mm by 300 mm composite plate. The 1st analysis was performed on a 1 mm thick CFRP plate, where carbon fibre was treated as a homogeneous material. The following 4 simulations utilised the ACP module to arrange the composite layers properly.

In these simulations, ten layers of carbon fibre, each 0.1 mm thick, were applied to the plate, maintaining a total thickness of 1 mm – identical to the 1st simulation. In the 2nd simulation, the fibres were oriented at 0°, in the 3rd at 90°, in the 4th at 30°, and in the final case at 45°. The material used for the plate was Epoxy Carbon UD (230 GPa) Wet, a material commonly employed in the hand lamination process, which is a typical method for manufacturing UAV components. Carbon Fibre UD refers to a type of material in which carbon fibres are aligned in a single direction. This configuration maximises the material's strength and stiffness along the axis of the fibres, providing high tensile strength and rigidity in that direction.

The analysed structure was converted into a shell model. The shell was assigned a thickness of 1 mm, with carbon fibre specified as a homogeneous material. When the ACP module was used, the thickness was determined by the cumulative thickness of the individual laminate layers. The element size was 5 mm, with the *Face Meshing* option applied. The surface was meshed using SHELL181 elements, which have 6 DOFs per node, totalling 24 DOFs (ANSYS Inc. 2010). The mesh consists of 6000 elements.

ANSYS software was used for the simulation-based modal analysis, with the primary motivation being the availability of the ACP module. This advanced tool facili-

tates composite structure modelling, analysis, and optimisation. The ACP module utilizes CLT, which is fundamental for understanding the behaviour of laminated composite structures. Simulating composite materials presents significant challenges due to their inherent structural complexity. Notably, composites are classified as orthotropic, meaning factors such as fibre orientation critically influence the strength and stiffness of the component under investigation.

The ACP module precisely defines material properties and configures the layers within the analysed laminate. Each layer is treated as a distinct entity, with the flexibility to assign unique material properties, fibre orientations, and thicknesses, enabling the creation of complex laminate structures. Furthermore, the module allows for the definition of mechanical, thermal, and electrical properties for each layer, supporting comprehensive multi-physics analysis. This functionality is crucial for capturing the complex behaviour of composite materials and ensuring simulation accuracy. A key feature of the ACP module is its capability to generate and modify complex layer configurations by specifying the sequence of layer arrangements. Optimizing the layer configuration helps maximize the strength-to-weight ratio, which is an essential criterion in aerospace. The accurate representation of fibre orientation is critical, as it directly influences the precision of simulation results. The module seamlessly integrates with other tools within the ANSYS environment, enabling comprehensive analyses across multiple domains. Once the composite layout is defined, the model can be transferred to other ANSYS tools for strength, flow, thermal, or modal analysis.

Table 1. Properties of used material

Property	Value
Density	1518 kg/m ³
Young's modulus X direction	123.34 GPa
Young's modulus Y direction	7.78 GPa
Young's modulus Z direction	7.78 GPa
Poisson's ratio XY	0.27
Poisson's ratio YZ	0.42
Poisson's ratio XZ	0.27
Shear modulus XY	5 GPa
Shear modulus YZ	3.08 GPa
Shear modulus XZ	5 GPa
Ultimate tensile strength X direction	1632 MPa
Ultimate tensile strength Y direction	34 MPa
Ultimate tensile strength Z direction	34 MPa
Ultimate compressive strength X direction	-704 MPa
Ultimate compressive strength Y direction	-68 MPa
Ultimate compressive strength Z direction	-68 MPa
Ultimate shear strength XY	80 MPa
Ultimate shear strength YZ	55 MPa
Ultimate shear strength XZ	80 MPa

Additionally, the ACP module supports failure strength analysis, addressing issues such as crack initiation or propagation. It employs composite-specific strength criteria, including Hashin, Puck, and Tsai-Wu, to accurately assess material performance under various loading conditions. The nonlinear analysis capabilities of ACP also allow for modelling large deformations and failure mechanisms like delamination, fibre fracture, and matrix cracking, which are essential for realistic simulations of composite material behaviour under extreme operational conditions. This functionality thoroughly evaluates composite structures, encompassing their mechanical integrity and failure mechanisms (Kaw 2005). Each composite layer is made from the material described in Table 1. As previously mentioned, 0°, 90°, 30°, and 45° stack-up sequences have been created from unidirectional carbon fibre.

The stack-up sequences of 0°, 90°, 30°, and 45° are shown in Figures 2–5. The directionality of the carbon fibre is defined compared to the horizontal X-axis.

It was decided to carry out a free – free analysis. That is, any boundary conditions do not constrain the object. The structure then has 6 DOFs in a 3-dimensional coordinate system. For the free-free analysis, the 1st 6 natural frequencies equal 0 or close to 0. These are the so-called rigid body modes. This means the whole structure can move rigidly, making 3 translational movements and 3 rotational movements without excitation. It was resolved to limit the analysis to detect 12 modes. The lowest frequency of interest was set to 0.5 Hz to avoid detection of rigid body modes.

4. Results

The natural frequencies for the individual simulations are summarised in Table 2.

The 1st 3 mode shapes are shown in Figures 6–8. The results indicate that the 1st mode shape for both the homogeneous material and the 90° fibre orientation is identical, corresponding to a purely bending mode. Additionally, the natural frequency values for these configurations are closely aligned. This similarity suggests that when fibres are aligned perpendicular to the main axis of deformation, the structure behaves similarly to a homogenous material, primarily resisting bending due to the uniform stiffness along the fibre direction. However, the analysis of subsequent mode shapes reveals no convergence between the homogeneous material and the 90° orientation in higher modes.

In Figure 7, the mode shapes for the 2nd natural frequency across all configurations are illustrated. This figure shows that, while the homogenous material and 90° fibre orientation continue to exhibit similar deflection patterns dominated by torsion, each of the other fibre orientations perform a more complex response. The 30° and 45° configurations display mixed bending – torsion modes. For fibres oriented at 0° bending modes are presented.

Figure 8 presents the mode shapes associated with the 3rd identified natural frequency, which are distinctly different. This lack of correspondence persists in the fol-

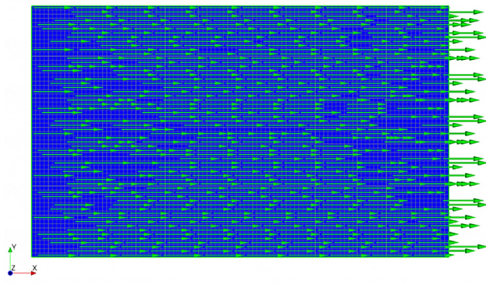
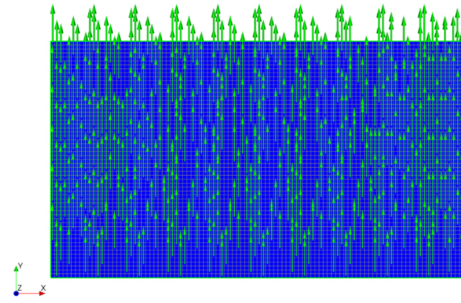
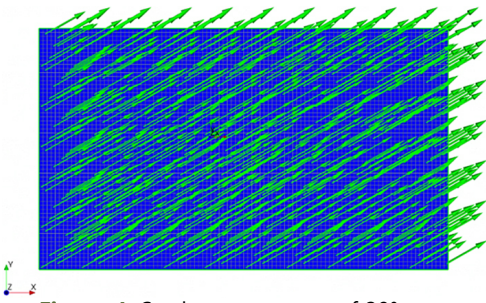
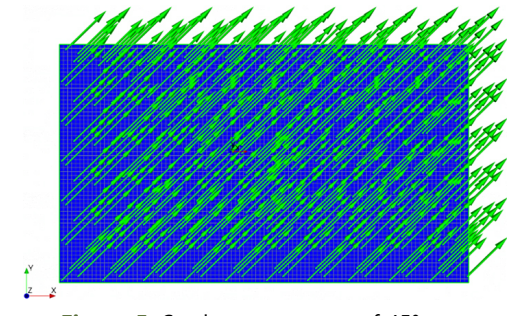
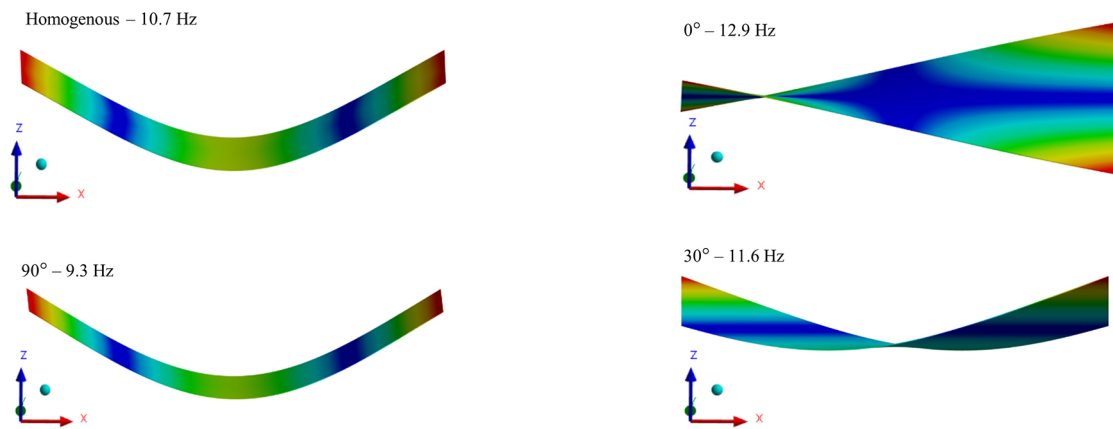
Figure 2. Stack-up sequence of 0° Figure 3. Stack-up sequence of 90° Figure 4. Stack-up sequence of 30° Figure 5. Stack-up sequence of 45° 

Figure 6. Mode shapes for 1st natural frequencies for all sequences

lowing mode shapes, where no similarities are observed between the 2 configurations. For fibres oriented at 90° , the 1st vibration mode is characterised by pure bending. The structure undergoes deflection, with dominant phenomena occurring in the plane perpendicular to the fibre direction, which is 90° relative to the X -axis. This behaviour results from the significantly higher stiffness of the material along the fibres, causing bending to be the primary mechanism of natural vibrations in the planes where the structure exhibits lower stiffness. In this case, the fibres primarily reinforce the structure in the direction perpendicular to the vibrations, leading to the characteristic behaviour of deflections. A similar pattern is observed for the homogeneous material. For fibres oriented at 0° , the 1st mode of natural vibrations manifests as torsion. Rotational movement occurs around a point located approximately 10% of the distance from the plate's shorter edge. This effect is due to the dominance of stiffness in the fibre

direction, which is aligned along the length of the plate, resulting in substantial resistance to bending. This case demonstrates that fibre orientation along the longer dimension shifts the dominant vibration mechanism from bending to twisting. With fibre orientations at 30° and 45° , the 1st mode of natural vibrations involves torsion around the centre of the plate. In this case, 2 opposite corners of the plate move upward while the others move downward, indicating a more complex interaction between longitudinal and transverse stiffness. Fibres arranged at these angles provide a more balanced stiffness distribution, leading to more symmetric torsional behaviour. The area around which rotational movement occurs shifts toward the centre of the plate, likely due to the intermediate fibre orientation, which does not dominate in either the longitudinal or transverse direction but instead provides balanced stiffness in both axes. The following figure graphically illustrates the natural frequencies for the various modes.

As shown in Figure 9, the effect of fibre orientation on the natural vibration frequencies within the next modes is evident for all twelve considered vibration frequencies. A direct comparison of changes in the vibration frequency values within a single mode, resulting from changes in the fibre alignment angle, is not justified due to significant

changes in the mode shapes visible in Figures 6 and 7. These changes indicate that fibre orientation not only influences frequency but also fundamentally alters the deformation pattern, making mode shapes analysis essential to understanding the structural dynamics fully.

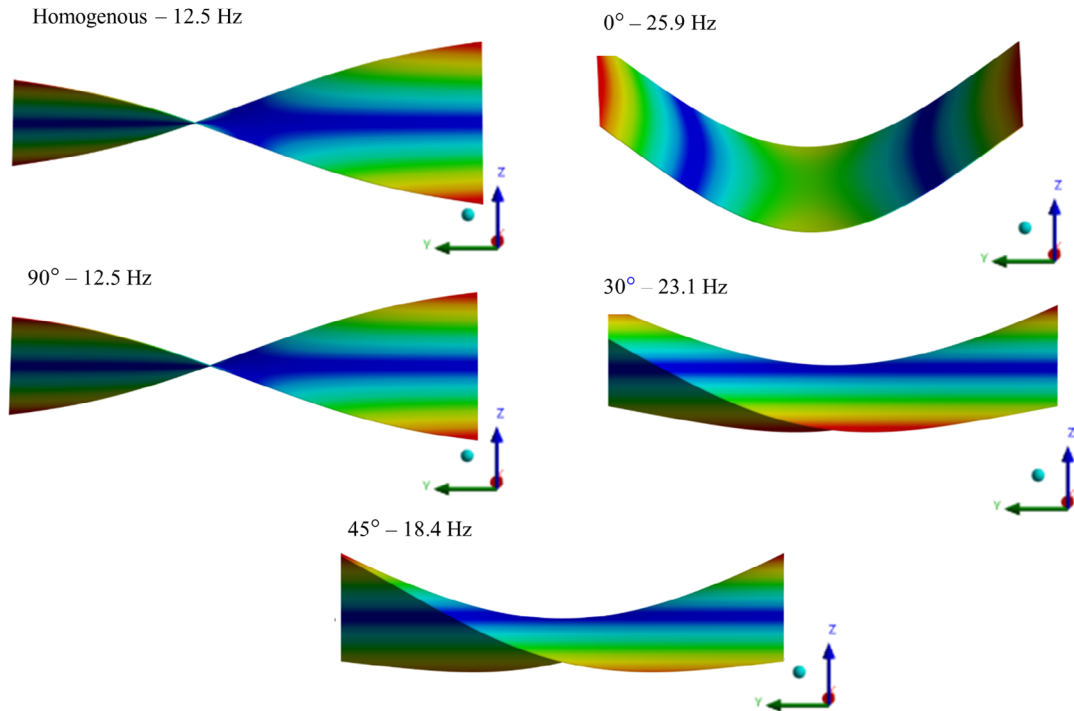


Figure 7. Mode shapes for 2nd natural frequencies for all sequences

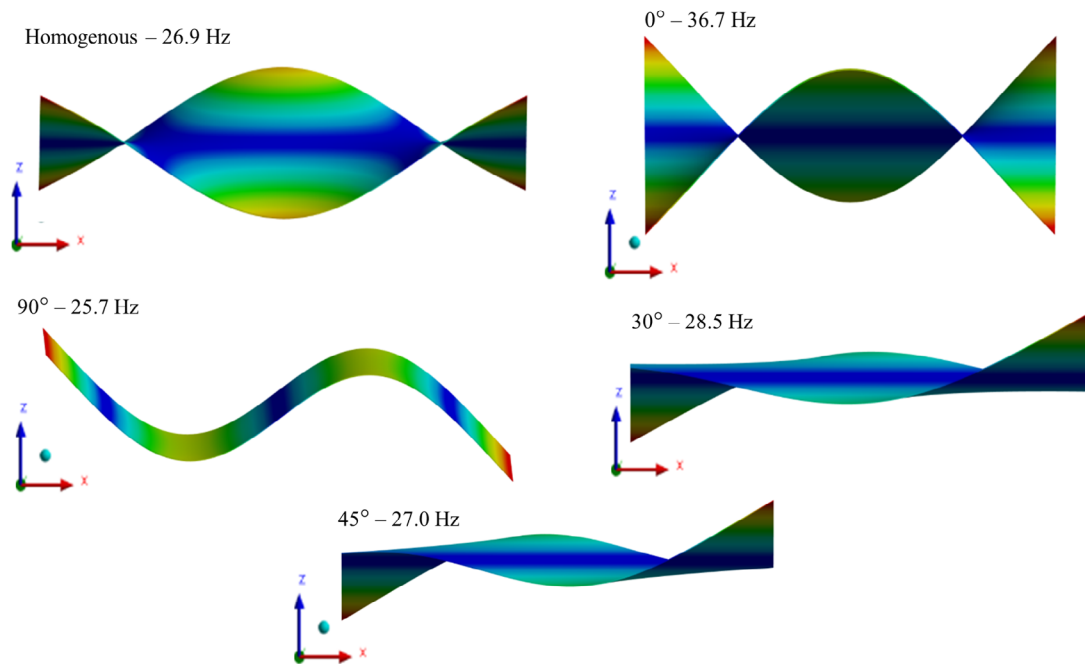
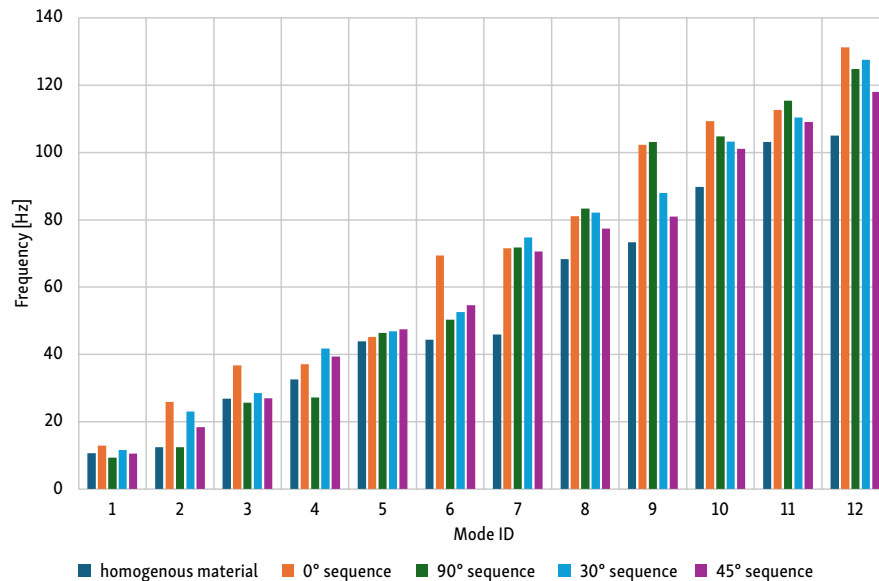


Figure 8. Mode shapes for 3rd natural frequencies for all sequences

Table 2. Natural frequencies values

Mode ID	Frequency [Hz]				
	Homogeneous	Sequence			
		0°	90°	30°	45°
1	10.7	12.9	9.3	11.6	10.6
2	12.5	25.9	12.5	23.1	18.4
3	26.9	36.7	25.7	28.5	27.0
4	32.6	37.2	27.2	41.7	39.3
5	43.9	45.2	46.4	46.9	47.5
6	44.4	69.5	50.4	52.6	54.6
7	45.9	71.5	71.8	74.8	70.6
8	68.4	81.1	83.4	82.2	77.4
9	73.3	102.4	103.2	88.0	80.9
10	89.7	109.3	104.8	103.2	101.2
11	103.1	112.7	115.4	110.4	109.2
12	105.1	131.2	124.9	127.5	118.1

**Figure 9.** Natural frequency values for all configurations

5. Conclusions and future work

This study aimed to conduct a simulation modal analysis for a composite plate with different fibre definitions and orientations. The simulation was performed using ANSYS software within the ACP environment. In the 1st model, the material was assigned to the plate from the library as a homogeneous material without considering fibre directionality. The next 4 models were prepared in the ACP module, with the fibres arranged at 0°, 90°, 30°, and 45° relative to the X-axis.

The results confirm that both the natural frequencies and mode shapes strictly depend on the fibres' orientation. Variations in the alignment direction lead to differences in the values of the natural frequencies, with particularly noticeable distinctions in mode shapes. This phenomenon occurs because the fibres carry most of the load

and impart stiffness to the structure; as the fibre direction changes, the structure becomes more susceptible to deformation in that direction.

Additionally, the study demonstrated that assigning a composite material to the entire structure without considering fibre directionality complicates the determination of the material's properties, making it difficult to relate to the other simulations. The homogenous assumption does not capture the orthotropic behaviour of composite materials, where stiffness and strength are heavily dependent on fibre orientation. As a result, such a model lacks real – world relevance for applications involving directional composites, as it cannot accurately predict the structural response to dynamic loads. From this study, it can be concluded that considering fibre directionality in the simulation modal analysis of composite materials is crucial for accurately representing the structural dynamics. Assigning

a composite material to a structure without accounting for fibre direction is not advisable. In carbon composites, the fibres are aligned in specific directions, while results obtained without considering directionality do not correspond to any actual orientation. These findings are significant for studying structural dynamics in UAVs. In the future, experimental tests will be conducted to validate the computational model and studies based on actual UAV structures.

References

- Addcomposites. 2024. *Composites in Urban Transport: Current Applications and Future Prospects*. Addcomposites Oy, Espoo, Finland. Available from Internet: <https://www.addcomposites.com/post/composites-in-urban-transport-current-applications-and-future-prospects>
- Anderson, K.; Gaston, K. J. 2013. Lightweight unmanned aerial vehicles will revolutionize spatial ecology, *Frontiers in Ecology and the Environment* 11(3): 138–146. <https://doi.org/10.1890/120150>
- ANSYS Inc. 2010. *ANSYS Meshing User's Guide: Release 13.0*. ANSYS Inc., Canonsburg, PA, US. 350 p.
- Bagdi, Z.; Csámer, L.; Bakó, G. 2023. The green light for air transport: sustainable aviation at present, *Cognitive Sustainability* 2(2): 1–7. <https://doi.org/10.55343/cogsust.55>
- Bishay, P. L.; Aguilar, C. 2021. Parametric study of a composite skin for a twist-morphing wing, *Aerospace* 8(9): 259. <https://doi.org/10.3390/aerospace8090259>
- Bras, M.; Warwick, S.; Suleman, A. 2022. Aeroelastic evaluation of a flexible high aspect ratio wing UAV: numerical simulation and experimental flight validation, *Aerospace Science and Technology* 122: 107400. <https://doi.org/10.1016/j.ast.2022.107400>
- Bubert, E. A.; Woods, B. K. S.; Lee, K.; Kothera, C. S.; Wereley, N. M. 2010. Design and fabrication of a passive 1D morphing aircraft skin, *Journal of Intelligent Material Systems and Structures* 21(17): 1699–1717. <https://doi.org/10.1177/1045389X10378777>
- Bushnaq, O. M.; Mishra, D.; Natalizio, E.; Akyildiz, I. F. 2022. Unmanned aerial vehicles (UAVs) for disaster management, in A. Denizli, M. S. Alencar, T. A. Nguyen, D. E. Motaung (Eds.), *Nanotechnology-Based Smart Remote Sensing Networks for Disaster Prevention*, 159–188. <https://doi.org/10.1016/B978-0-323-91166-5.00013-6>
- Chajec, W. 2020. *Aeroelastyczność samolotów i szybowców w praktyce*. Biblioteka Naukowa Instytutu Lotnictwa, Warszawa. 311 s. (in Polish).
- Chajec, W. 2018. Methods of modern aircraft aeroelastic analyses in the institute of aviation, *Journal of KONES Powertrain and Transport* 25(4): 33–42. Available from Internet: https://kones.eu/ep/2018/vol25/no4/33-42_J_O_KONES_2018_NO_4_VOL_25_ISSN_1231-4005_CHAJEC.pdf
- Ciampa, E.; De Vito, L.; Pecce, M. R. 2019. Practical issues on the use of drones for construction inspections, *Journal of Physics: Conference Series* 1249: 012016. <https://doi.org/10.1088/1742-6596/1249/1/012016>
- Colomina, I.; Molina, P. 2014. Unmanned aerial systems for photogrammetry and remote sensing: a review, *ISPRS Journal of Photogrammetry and Remote Sensing* 92: 79–97. <https://doi.org/10.1016/j.isprsjprs.2014.02.013>
- Dagilis, M.; Kilikevičius, S. 2023. Aeroelasticity model for highly flexible aircraft based on the vortex lattice method, *Aerospace* 10(9): 801. <https://doi.org/10.3390/aerospace10090801>
- Davies, G. A. O.; Zhang, X. 1995. Impact damage prediction in carbon composite structures, *International Journal of Impact Engineering* 16(1): 149–170. [https://doi.org/10.1016/0734-743X\(94\)00039-Y](https://doi.org/10.1016/0734-743X(94)00039-Y)
- Dinulović, M.; Bengin, A.; Krstić, B.; Dodić, M.; Vorkapić, M. 2024. Flutter optimization of carbon/epoxy plates based on a fast tree algorithm, *Aerospace* 11(8): 636. <https://doi.org/10.3390/aerospace11080636>
- Evins, D. J. 2000. *Modal Testing: Theory, Practice and Application*. 2nd Edition. Wiley. 592 p.
- Ficzere, P. 2022. The impact of the positioning of parts on the variable production costs in the case of additive manufacturing, *Periodica Polytechnica Transportation Engineering* 50(3): 304–308. <https://doi.org/10.3311/PPtr.15827>
- Friswell, M. I.; Mottershead, J. E. 1995. *Finite Element Model Updating in Structural Dynamics*. Springer. 292 p. <https://doi.org/10.1007/978-94-015-8508-8>
- Garrick, I. E.; Reed, W. H. 1981. Historical development of aircraft flutter, *Journal of Aircraft* 18(11): 897–912. <https://doi.org/10.2514/3.57579>
- George, J. S.; Vasudevan, A.; Mohanavel, V. 2021. Vibration analysis of interply hybrid composite for an aircraft wing structure, *Materials Today: Proceedings* 37: 2368–2374. <https://doi.org/10.1016/j.matpr.2020.08.078>
- Gibson, R. F. 2016. *Principles of Composite Material Mechanics*. 4th Edition. CRC Press. 700 p. <https://doi.org/10.1201/b19626>
- Gondaliya, R.; Sypeck, D.; Zhu, F. 2016. Improving damage tolerance of composite sandwich structure subjected to low velocity impact loading: experimental analysis, in *Proceedings of the American Society for Composites 2016 – Thirty-First Technical Conference on Composite Materials*, 19–22 September 2016, Williamsburg, VA, US, 1–17. Available from Internet: <https://www.dpi-proceedings.com/index.php/asc31/article/view/3128>
- Hausamann, D.; Zirinig, W.; Schreier, G.; Strobl, P. 2005. Monitoring of gas pipelines – a civil UAV application, *Aircraft Engineering and Aerospace Technology* 77(5): 352–360. <https://doi.org/10.1108/00022660510617077>
- Herrick, K. 2000. Development of the unmanned aerial vehicle market: forecasts and trends, *Air & Space Europe* 2(2): 25–27. [https://doi.org/10.1016/S1290-0958\(00\)80035-0](https://doi.org/10.1016/S1290-0958(00)80035-0)
- Hodges, D. H.; Pierce, G. A. 2011. *Introduction to Structural Dynamics and Aeroelasticity*. 2nd Edition. Cambridge University Press. 247 p. <https://doi.org/10.1017/CBO9780511997112>
- ICAO. 2011. *Unmanned Aircraft Systems (UAS)*. ICAO Cir 328. International Civil Aviation Organization (ICAO), Montreal, QC, Canada. 54 p. Available from Internet: https://www.icao.int/meetings/uas/documents/circular%20328_en.pdf
- Kaw, A. K. 2005. *Mechanics of Composite Materials*. 2nd Edition. CRC Press. 490 p. <https://doi.org/10.1201/9781420058291>
- Karpenko, M. 2022. Landing gear failures connected with high-pressure hoses and analysis of trends in aircraft technical problems, *Aviation* 26(3): 145–152. <https://doi.org/10.3846/aviation.2022.17751>
- Karpenko, M.; Nugaras, J. 2022. Vibration damping characteristics of the cork-based composite material in line to frequency analysis, *Journal of Theoretical and Applied Mechanics* 60(4): 593–602. <https://doi.org/10.15632/jtam-pl/152970>
- Karpenko, M.; Stosiak, M.; Deptuła, A.; Urbanowicz, K.; Nugaras, J.; Królczyk, G.; Żak, K. 2023. Performance evaluation of extruded polystyrene foam for aerospace engineering applications using frequency analyses, *The International Journal of Advanced Manufacturing Technology* 126(11–12): 5515–5526. <https://doi.org/10.1007/s00170-023-11503-0>

- Kidane, B. S.; Troiani, E. 2020. Static aeroelastic beam model development for folding winglet design, *Aerospace* 7(8): 106. <https://doi.org/10.3390/aerospace7080106>
- Kollár, L. P.; Springer G. S. 2003. *Mechanics of Composite Structures*. Cambridge University Press. 480 p. <https://doi.org/10.1017/CBO9780511547140>
- Kontogiannis, S. G.; Ekaterinaris, J. A. 2013. Design, performance evaluation and optimization of a UAV, *Aerospace Science and Technology* 29(1): 339–350. <https://doi.org/10.1016/j.ast.2013.04.005>
- Koottatep, T.; Winijkul, E.; Xue, W.; Panuvatvanich, A.; Visvanathan, C.; Pussayanavin, T.; Limphitakphong, N.; Polprasert, C. 2023. *Marine Plastics Abatement: Technology, Management, Business and Future Trends*. Volume 2. IWA Publishing. <https://doi.org/10.2166/9781789063448>
- Koukoudakis, G. 2024. Drones' contribution to the transformation of contemporary warfare, *Journal of Military Studies* 13(1): 24–32. <https://doi.org/10.2478/jms-2024-0003>
- Kovalev, I. V.; Voroshilova, A. A.; Karaseva, M. V. 2019. Analysis of the current situation and development trend of the international cargo UAVs market, *Journal of Physics: Conference Series* 1399(5): 055095. <https://doi.org/10.1088/1742-6596/1399/5/055095>
- Körpe, D. S.; Kanat, Ö. Ö. 2019. Aerodynamic optimization of a UAV wing subject to weight, geometric, root bending moment, and performance constraints, *International Journal of Aerospace Engineering* 2019: 3050824. <https://doi.org/10.1155/2019/3050824>
- Lyu, M.; Zhao, Y.; Huang, C.; Huang, H. 2023. Unmanned aerial vehicles for search and rescue: a survey, *Remote Sensing* 15(13): 3266. <https://doi.org/10.3390/rs15133266>
- Malinowski, Z. 2016. The role of unmanned aerial vehicles in the formation of a secure military supply chain, *Security and Defence Quarterly* 12(3): 19–45. <https://doi.org/10.35467/sdq/103235>
- Mallick, P. K. 2007. *Fiber-Reinforced Composites: Materials, Manufacturing, and Design*. 3rd Edition. CRC Press. 638 p. <https://doi.org/10.1201/9781420005981>
- Nettles, A. T. 1994. *Basic Mechanics of Laminated Composite Plates*. NASA Reference Publication No 1351. National Aeronautics and Space Administration (NASA), Marshall Space Flight Center (MSFC), AL, US. 107 p. Available from Internet: <https://ntrs.nasa.gov/api/citations/19950009349/downloads/19950009349.pdf>
- Noman, A. A.; Shohel, S. M.; Riyad, H. S.; Gupta, S. S. 2023. Investigate the mechanical strength of laminated composite carbon fiber with different fiber orientations by numerically using finite element analysis, *Materials Today: Proceedings* (in press). <https://doi.org/10.1016/j.matpr.2023.02.132>
- Panopoulou, A.; Loutas, T.; Roulias, D.; Fransen, S.; Kostopoulos, V. 2011. Dynamic fiber Bragg gratings based health monitoring system of composite aerospace structures, *Acta Astronautica* 69(7–8): 445–457. <https://doi.org/10.1016/j.actaastro.2011.05.027>
- Patil, M. J. 2003. Nonlinear aeroelastic analysis of joined-wing aircraft, in *44th AIAA/ASME/ASCE/AHS/ASC Structures, Structural Dynamics, and Materials Conference*, 7–10 April 2003, Norfolk, VA, US, 1–7. <https://doi.org/10.2514/6.2003-1487>
- Pálfi, T.; Ficzer, P. 2025. Aerodynamic study of different types of wingtip devices, *Periodica Polytechnica Transportation Engineering* 53(1): 77–86. <https://doi.org/10.3311/PPtr.37240>
- Piccione, E.; Bernardini, G.; Gennaretti, M. 2012. Structural-aeroelastic finite element modeling for advanced-geometry rotor blades, *Aircraft Engineering and Aerospace Technology* 84(6): 367–375. <https://doi.org/10.1108/00022661211272873>
- Qaumi, T.; Hashemi, S. M. 2023. Experimental and numerical modal analysis of a composite rocket structure, *Aerospace* 10(10): 867. <https://doi.org/10.3390/aerospace10100867>
- Rahmani, B.; Mortazavi, F.; Villemure, I.; Levesque, M. 2013. A new approach to inverse identification of mechanical properties of composite materials: regularized model updating, *Composites Structures* 105: 116–125. <https://doi.org/10.1016/j.compstruct.2013.04.025>
- Rangappa, S. M.; Parameswaranpillai, J.; Siengchin, S.; Kroll, L. 2020. *Lightweight Polymer Composite Structures: Design and Manufacturing Techniques*. CRC Press. 410 p. <https://doi.org/10.1201/9780429244087>
- Rango, A.; Laliberte, A.; Herrick, J. E.; Winters, C.; Havstad, K.; Steele, C.; Browning, D. 2009. Unmanned aerial vehicle-based remote sensing for rangeland assessment, monitoring, and management, *Journal of Applied Remote Sensing* 3(1): 033542. <https://doi.org/10.1117/1.3216822>
- Rose, R. A.; Byler, D.; Eastman, J. R.; Fleishman, E.; Geller, G.; Goetz, S.; Guild, L.; Hamilton, H.; Hansen, M.; Headley, R.; Hewson, J.; Horning, N.; Kaplin, B. A.; Laporte, N.; Leidner, A.; Leimgruber, P.; Morissette, J.; Musinsky, J.; Pintea, L.; Prados, A.; Radeloff, V. C.; Rowen, M.; Saatchi, S.; Schill, S.; Tabor, K.; Turner, W.; Vodacek, A.; Vogelmann, J.; Wegmann, M.; Wilkie, D.; Wilson, C. 2015. Ten ways remote sensing can contribute to conservation, *Conservation Biology* 29(2): 350–359. <https://doi.org/10.1111/cobi.12397>
- Schaff, J. R.; Davidson, B. D. 1997. Life prediction methodology for composite structures. Part I – constant amplitude and two-stress level fatigue, *Journal of Composite Materials* 31(2): 128–157. <https://doi.org/10.1177/002199839703100202>
- Siemens. 2022. *Aircraft Ground Vibration Testing: Enhancing the Efficiency of Aircraft Structural Dynamics Testing*. Siemens Digital Industries Software. 9 p. Available from Internet: https://www.plm.automation.siemens.com/media/global/en/Siemens%20SW%20Aircraft%20ground%20vibration%20testing%20White%20Paper_tcm27-84865.pdf
- Silva, W. 2007. Recent enhancements to the development of CFD-based aeroelastic reduced-order models, in *48th AIAA/ASME/ASCE/AHS/ASC Structures, Structural Dynamics, and Materials Conference*, 23–26 April 2007, Honolulu, HI, US, 1–11. <https://doi.org/10.2514/6.2007-2051>
- Stosiak, M.; Karpenko, M.; Deptuła, A. 2022. Coincidence of pressure pulsations with excitation of mechanical vibrations of hydraulic system components: an experimental study, *Cognitive Sustainability* 1(2): 12. <https://doi.org/10.55343/cogsust.12>
- Tremaine, K. 2012. *Modal Analysis of Composite Structures with Damping Material*. MSc Thesis. California Polytechnic State University, San Luis Obispo, CA, US. 130 p. <https://doi.org/10.15368/theses.2012.139>
- Weisshaar, T.; Nam, C.; Batista-Rodriguez, A. 1998. Aeroelastic tailoring for improved UAV performance, in *39th AIAA/ASME/ASCE/AHS/ASC Structures, Structural Dynamics, and Materials Conference and Exhibit*, 20–23 April 1998, Long Beach, CA, UA, 1–13. <https://doi.org/10.2514/6.1998-1757>
- Zhang, C.; Kovacs, J. M. 2012. The application of small unmanned aerial systems for precision agriculture: a review, *Precision Agriculture* 13: 693–712. <https://doi.org/10.1007/s11119-012-9274-5>
- Zrelli, I.; Rejeb, A.; Abusulaiman, R.; Al Sahafi, R.; Rejeb, K.; Iranmanesh, M. 2024. Drone applications in logistics and supply chain management: a systematic review using latent Dirichlet allocation, *Arabian Journal for Science and Engineering* 49(9): 12411–12430. <https://doi.org/10.1007/s13369-023-08681-0>